(Article begins on next page)

A Novel Tool for Predicting Extracapsular Extension During Graded Partial Nerve Sparing in Radical Prostatectomy

Patel Vipul[1], Sandri Marco[2], Grasso Angelica Anna Chiara[3], De Lorenzis Elisa[3], Palmisano Franco[3], Albo Giancarlo[3], Coelho Rafael Ferreira[4], Mottrie Alexander[5], Harvey Tadzia[1], Kameh Darian[1], Palayapalayam, Hariharan[1], Wiklund Peter[6], Bosari Silvano[7], Puliatti Stefano[9], Zuccolotto Paola[8], Bianchi Giampaolo[9], Rocco Bernardo[9-1]

[1] Global Robotics Institute, Florida Hospital-Celebration Health Celebration, University of Central Florida School of Medicine, Orlando, FL, USA

[2] Data Methods and Systems Statistical Laboratory, University of Brescia, Brescia, Italy

[3] Department of Urology, Fondazione IRCCS Ca' Granda-Ospedale Maggiore Policlinico, University of Milan, Milan, Italy

[4] Department of Urology, Instituto do Cancer, Universidade de Sao Paulo Faculdade de Medicina Hospital das Clinicas, Sao Paulo, SP, Brazil

[5] Department of Urology, Onze-Lieve-Vrouw Hospital, Aalst, Belgium; OLV Vattikuti Robotic Surgery Institute, Melle, Belgium

[6] Department of Urology, Karolinska University Hospital, Stockholm, Sweden

[7] Division of Pathology, Fondazione IRCCS Ca' Granda, Ospedale Maggiore

Policlinico, Milan, Italy

[8] Big&Open Data Innovation Laboratory University of Brescia, Brescia, Italy

[9] Department of Urology, Ospedale Policlinico e Nuovo Ospedale Civile

S.Agostino Estense Modena, University of Modena and Reggio Emilia,

Modena, Italy

CORRESPONDING AUTHOR

Bernardo Rocco M.D
Associate Professor of Urology
University of Modena and Reggio Emilia
Department of Urology
Nuovo Ospedale Civile S.Agostino Estense
Via Pietro Giardini 1355 - 41126 Modena
Tel +390593961036
Email: bernardo.rocco@gmail.com

Abstract:

OBJECTIVES

To create a statistical tool for the estimation of extra-capsular extension (ECE) level of prostate cancer

and determine the nerve sparing (NS) approach that can be safely performed during radical

prostatectomy (RP).

PATIENTS AND METHODS

A total of 11,794 lobes, from 6,360 patients who underwent robot¬ assisted RP between 2008 and

2016 were evaluated. Clinicopathological features were included in a statistical algorithm for the

prediction of the maximum ECE width. Five multivariable logistic models were estimated for:

presence of ECE and ECE width greater than 1, 2, 3, and 4mm. A five¬ zone decision rule based on a

lower and upper threshold is proposed. Using a graphical interface, surgeons can view a patient's pre-

treatment characteristics and a curve showing the estimated probabilities for ECE amount and the areas identified by the decision rule.

RESULTS

Out of 6,360 patients, 1,803 (28.4%) were affected by non-organ-confined disease. ECE was present in 1,351 lobes (11.4%) and extended beyond the capsule for more than 1, 2, 3, and 4mm in 498 (4.2%), 261 (2.2%), 148 (1.3%), 99 (0.8%) cases, respectively. ECE width was up to 15 mm (IR 1.00 - 2.00). The 5 logistic models showed good predictive performance; the area under the ROC curve was: 0.81 for ECE, and 0.84, 0.85, 0.88, and 0.90 for ECE width greater than 1, 2, 3, and 4mm, respectively.

CONCLUSION

This novel tool predict with a good accuracy the presence and amount of ECE. Furthermore, the graphical interface available at www.prece.it can supports surgeons in patient counselling and preoperative planning.

Introduction

The introduction of nerve-sparing (NS) radical prostatectomy (RP) in 1983 improved the potency and continence outcomes in treatment of clinically localized prostate cancer (PCa).[1,2] While preservation of the neurovascular bundle (NVB) improves the chance of recovering erectile function, it may lead to an increased incidence of positive surgical margins (PSM).[3] To maximize the functional outcome while maintaining quality of cancer care, the NS approach has changed from an absolute ("all-or-none") approach to a graded approach.

According to our prior publication we proposed that NS can be graded into 5 levels, depending on the amount of tissue the surgeon decides to leave on each side.[4,5] Various papers have shown that NS classification according to

the surgeon's intraoperative perception correlates with the residual nerve tissue found on specimens.[6-9]

Knowledge of the presence and extent of extra-capsular extension (ECE) before surgery would help surgeons tailor the amount of NS. Several tools can predict the presence of ECE or other outcomes, most of them are based on routinely available variables.[10-13] However, to our knowledge, there are no algorithms supporting preoperative planning, with a quantification not only of the presence of ECE, but of the amount of ECE; this information is crucial in order to make an appropriate, standardized decision between a full NS, a partial NS, or a wide excision.

The aims of the present study were threefold: to describe the amount of ECE; to develop a predictive model of the presence and amount of ECE; to develop a decision rule to assist the surgeon in the trade-off between NVB preservation and absence of PSM.

Patients and methods

A total of 11,794 prostatic lobes, from a cohort of 6,360 patients who underwent robot assisted laparoscopic prostatectomy (RALP) between January 2008 and January 2016 by a single surgeon were evaluated.

No centralized revision of the core biopsies have been done; only those patients with less than 5% of disease and one positive core were reviewed by a single expert pathologist (DK) (2.8%). As far as the final prostate specimen is concerned, after a proper processing, the slides were examined for the presence of ECE. ECE is defined as the presence of tumor beyond the confines of the prostate,[14] independently from the seminal vesicle involvement, that is not matter of our investigation. The maximum continuous

length of ECE was recorded, along with its "width" (perpendicular dimension from capsule to furthest extent of ECE). At other locations, where the prostatic capsule was not evident, a best estimation was made concerning the distance of invasion into periprostatic soft tissue. Patients with less than 3 cores per lobe (3.3%) or pre-operative medical therapies such as hormone (2.2%) or 5α-Reductase inhibitors (0.6%) were excluded; globally 408 patients were excluded (6%).

The predictive algorithm

The building blocks of the proposed prediction algorithm are shown in Figure 1. The algorithm was built with the aim of predicting different degrees of extracapsularity for each lobe. Five binary outcomes were considered: the presence of ECE and ECE width greater than 1, 2, 3, and 4mm. We decided to focus our prediction in the range from 0 to 4mm because in our cohort more than 95% of pT3 disease had ECE within 5mm.

Variable selection

The list of preoperative characteristics considered as potential predictors of ECE and used in the variable selection were recorded in Table S1.

The selection of the predictive covariates was performed using the AUC-RF algorithm[15] which maximizes the area under the receiver operating characteristic curve (AUC) of random forests.[16] Its advantage is the ability to evaluate the predictive power of each covariate individually as well as in multivariate interactions with other predictors.[17]

Model estimation

The covariates selected as predictors were used as explanatory variables in the estimation of the multivariable logistic regression models for the five ECE outcomes. The goodness of fit of these models was investigated using calibration curves which evaluate the agreement between observed and predicted probabilities. The predictive power of the models was evaluated estimating sensitivity and specificity for different thresholds on the predicted probabilities, plotting the receiver operating characteristic (ROC) curve and calculating the AUC. The AUC was also estimated using repeated k-fold cross-validation.

Personal profile plot

The predictions yielded by the five regression models were used to draw for each patient and each lobe a personal profile plot which shows the predicted probabilities for different ECE widths.

Decision rule

For each amount of ECE a five-zone decision rule was developed (the *multi limen* rule, henceforth) (Figure S1)[18]; four thresholds were estimated for each model: an upper and an uppermiddle threshold corresponding to a maximum rate of false positives (FP) of 10% and 20%, respectively, a lower and a lowermiddle threshold corresponding to a maximum rate of false negatives (FN) of 10% and 20%, respectively. Overall, the decision rule works using a set of 20 thresholds. The aim of these thresholds is to classify each estimated probability of ECE width into five areas: a green and a light green zone characterized respectively by low and medium rates of FN, a light red and a red zone characterized by medium and low rates of FP, and a yellow

intermediate zone with higher rates of decision errors. In the green and red zones, the decision rule provides suggestions to the surgeon regarding the boundaries of the resection. In the yellow zone additional diagnostic tools (e.g., mpMRI) might be advisable and the surgical strategy should be evaluated more carefully.

Graphical interface

In order to make this tool easily accessible, a user-friendly graphical interface was developed. Using this tool the surgeon can view all the patient's main pre-treatment information, together with the plot of estimated probabilities for different amounts of ECE and the *multi limen* decision rule.

Results

Clinical and pathological characteristics of study population are summarized in Table 1. According to the D'Amico classification, 2,737(43.0%), 2,684(42.2%), and 939(14.8%) patients were in the low, intermediate, and high risk group, respectively. ECE width was up to 15mm, with a median value of 1.0mm and an interquartile range (IQR) of 1.0 to 2.0mm. 97.6% of pT3 patients has ECE within 5 mm and the risk of ECE is virtually absent beyond 10mm outside of the prostate; The spatial distribution of ECE is represented in Figure S2. The median value of ECE length was 3.0mm (IQR=1.0 - 7.0mm, range 0.1 - 40.0mm). In 1,876(15.9%) lobes the number of core samples is between 3 and 5, in 9,106 lobes(77.2%) the cores were 6, and in 812(6.9%) they were more than 6.

Variable selection

Table S2 shows the univariate analysis of the association between clinical-pathological characteristics and the frequency of lobes with ECE and with

ECE width greater than 1, 2, 3, and 4mm. The data reported showed increasing values of ECE widths for increasing levels of age, PSA, clinical stage, percentage of positive cores, maximum percentage of positive core, and Gleason score. All these associations were statistically significant (P<0.001).

Variable selection identified 7 predictors of ECE: age, total PSA (logarithm), clinical stage, average percentage of cancer, ratio of number of cores with percentage of cancer greater than 60% and number of positive cores, ratio of number of cores with Gleason score greater than 6 and number of positive cores, rate of positive cores. The last two variables did not enter the models for ECE widths greater than 2, 3 and 4mm.

Model estimation

Table 2 records the multivariable odds ratios (ORs) of the 7 selected variables for each logistic model; positive and statistically significant associations between outcomes and predictors were found (P ranging from <0.001 to 0.029). The coefficients of the logistic models were reported in Table S3.

The calibration curve of the regression model used to predict the presence of ECE is shown in Figure 2. The bias-corrected curve, close to the straight line of the ideal predictor, showed that the probabilities calculated with this model accurately reproduce the actual outcomes. Figure S3 shows the calibration curves of the remaining models.

ROC curves of the regression model and their AUC are listed in Figure 3. All the models showed good predictive performances with AUC ranging from

0.81 to 0.90 (P<0.001). These results were confirmed by repeated (100 replications) 10-fold cross-validation (Table S4).

Personal profile plot

Probabilities of ECE widths were calculated for each patient. An example is presented in Figure S4.

Decision rule

At each step of the decision process the thresholds characterized by maximum FN and FP decision errors of 10% and 20% were calculated. The set of 20 thresholds are recorded in Table S5. Application of the decision rule to the predicted probabilities leads to the classification of each ECE probability into one of the five zones characterized by different levels of decision errors. An example is depicted in Figure S5. Risk comparison between the five zones identified by the decision rule was shown in Figures S6 and S7.

Graphical interface

All the relevant information regarding a patient, the profile plots for the two lobes and the areas defined by the *multi limen* decision rule were summarized by a graphical interface (Figure 4). The output includes 4 panels. The top left panel is subdivided into 12 coloured boxes; every box represents a biopsy core in its location (e.g. top left, first raw: LLA= left lateral apex) and reports the number, percentage and location of positive cores. The colours, from green to red, represent a progressive involvement of the cores. The top right panel is subdivided into 12 boxes and reports the Gleason Score of every core. The colours represent increasing Gleason scores. The bottom panels represent by coloured dots the five probabilities of different amounts of

ECE for the two lobes; the X axis reports the millimetres out of the prostatic capsule, the Y axis the probabilities. In the background of the two panels, 5 different areas are visualized according to different error levels of prediction. The colours of the dots are defined by the decision rule.

Figure 4 shows the output yielded by the graphical user interface for a 72-years-old patient with T2a clinical stage and PSA of 3ng/mL. The left lobe had no positive cores, while the right lobe had three positive cores all with Gleason score of 7. For the left lobe, the probability of ECE was 4.7% and was located inside the light green area; the probabilities of ECE>1, 2, 3 and 4mm were 2.1%, 1.0%, 0.4% and 0.3%, respectively, all inside the green area. Hence, the *multi limen* rule gave a indication of a full NS. For the right lobe, the five ECE probabilities were 46.7% (red), 20.5% (light red), 7.9% (yellow), 3.6% and 3.2% (light green), respectively. The decision rule suggested to avoid full NS, evidenced a consistent risk of ECE>1mm, and a moderated risk of ECE above 3mm. The final pathology revealed intracapsular disease on the left side and 2mm of ECE on the right.

Other examples are shown in Figures S8 and S9.

Web-based accessibility

In order to facilitate the use of the proposed prediction method, we set up an easy-to-use web-based interface, freely available at the link www.prece.it . On this website, the user can input the data of his/her patient and get the prediction of amount and side of ECE.

Discussion

ECE is found on pathologic analysis of PCa specimens in a significant number of patients with pre-operatively clinically localized PCa who undergo

RALP.[19-20] Maubon T et al.[21] report that not only the presence, but even the amount of ECE is an independent predictive factor of BCR. Wheeler et al. reported a rate of BCR of 13% in 5 years in patients with organ confined PCa, whereas in patients with local ECE the rate was as high as 27%.[22] In the same study, ECE was reported as an independent predictor for BCR.

Based on this background, it would be valuable to assess the risk of ECE before surgery to make decisions regarding the balance between cancer control and functional recovery. Furthermore, the introduction of robotic surgery has led to new idea in terms of NS: from an "all-or-none" to a more graded approach. In 2012 we reported a subjective graded approach to NS divided into 5 different levels.[5] This graded concept was opposed to an all-or-nothing approach, the attempt was to estimate the level of ECE and spare the amount of the NVB appropriate enough to excise the cancer but maximally preserve functional neurovascular tissue. However, so far, it has not been possible to standardize the decision-making process on when to take a more or less conservative approach.

Predictive tools available till now and new imaging techniques only partially support the process. Particularly, nomograms based on clinico-pathological features usually perform better than any individual predictive factor, informed clinical judgment, or easy-to-remember tools such as risk groups.[22,24] Preoperative factors are used in several nomograms as reliable predictors of ECE; Ohori's and Steuber's groups[25,26], among others, developed algorithms predicting the presence and side of ECE, the former based on 763 patients, with an AUC ranging from 0.78 to 0.80, the latter on 1118 patients and a C-index of 84%. These nomograms should support the surgeon in performing a

wider excision. However, they calculate a probability of ECE, but no decision rule and neither a prediction of the amount of ECE is provided. In other words, it is hard to decide when and how wide performing a dissection in the peri-prostatic tissue based on generic percentage of risk of ECE.

On the other hand, mpMRI is increasingly used for PCa imaging; as a support for target biopsies and to determine the extension of the PCa. Furthermore, mpMRI, has been investigated for its possible role in local staging. However, according to a recent meta-analysis published on a total of 75 studies (9796 patients) the overall sensitivity and specificity for the detection of ECE were only 0.57 (95% CI 0.49–0.65) and 0.91 (95% CI 0.88–0.93), respectively[27] (even though, MRI and clinical-based models combined may improve prediction of non organ confined disease, particularly for ECE and SVI)[28-30]. As a consequence, surgeons usually base their decision on preoperative variables and intraoperative visual clues[31]; however, this is far from being a safe, standardized and reproducible approach.

To address these issues, we evaluated the concept of amount of ECE and developed a model capable to predict with a good accuracy not only the presence but even the extent of ECE in patients subjected to RALP. In addition, we developed a decision rule to assist surgeons in their decision-making process. The graphical tool and the *multi limen* rule provide a simple visual clue of the predicted ECE, with a clear indication of the error level associated to the prediction.

We have previously described the landmark artery, a branch of the pudendal artery can be used anatomically to grade the amount of NS.[4] However, notwithstanding the accurate description of the anatomical landmark

considered in the differentiation of the type of NS[5], it might not be easy, particularly for less experienced surgeons, to identify such specific landmarks. Therefore, the prediction in terms of millimeters of ECE might be of help to plan the width of dissection, even without identifying specific anatomical landmarks of the NS.

The decision to define prediction between 0 and >4 mm out of the prostatic capsule is related to the fact that in the present cohort, 97.6% of the patients had disease within 5 mm.

It is worth to point out that the proposed prediction system is not intended to replace individualized clinician patient decision making, but rather to provide a straightforward instrument to facilitate ECE probability assessment.

Our study has several noteworthy strengths.

- The high sample size.
- The adoption of an approach that goes beyond the prediction of the presence of ECE; focusing on the estimation of probabilities of ECE width greater than 1, 2, 3, and 4mm, the proposed predictive algorithm yields for each patient and each prostate lobe a graph of the probabilities regarding the presence and amount of ECE.
- Unlike previous studies, our tool provides a decision rule integrated in an interface to make interpretation of outcomes easy for surgeons.
- The availability of an easy-to-use, free, web-based interface
- The diffusion of this tool might improve standardization and comparability of future studies in terms of PSM.
- The tool highlights the importance of millimetre-level ECE measurement. Although the prognostic role of accurate ECE

measurement is unclear[21] it might be useful in order to appropriately compare different series (e.g., the PSM percentage in a series with 1mm median ECE, might be lower compared to a series with 3mm median ECE, and this should be related to intrinsic patient characteristics rather than surgical issues).

The study has some limitations.

- The models have been developed and calibration has been performed; nevertheless, an external validation is needed to confirm the quality of the predictions and the reproducibility of the tool.

- The five models showed predictive performances that ranged from good to excellent according to the AUC. Nevertheless, the proposed predictive tool is based only on clinical-pathological factors and this could limit the accuracy of the models. Several recent studies have assessed the value of preoperative MRI in patients for evaluation of ECE[31-35], suggesting that prediction accuracy may be increased by integrating radiological information into predictive models; further prospective studies are needed to integrate our model with imaging tools.

- In addition, the study is based on a North American cohort from a single Institution, with limited number of afro-american patients and several caucasians; a geographic bias may affect the generalizability of our findings. Even though Steuber et al.[26] showed that multivariate nomograms on side specific ECE and their predictions are relatively unaffected by population differences, an external validation with different racial/ethnic groups is advisable in the future.

- Moreover, the population of the study is mostly low risk tumors (43%) with a relatively limited high risk patients.

To our knowledge, the present study is the first to propose an evidence based statistical tool that can be used to predict not only the presence but even the amount of ECE in prostate cancer specimens. This tool demonstrated good accuracy and, thanks to its user-friendly decision rule, can provide valuable assistance to surgeons in their preoperative planning.

In our algorithm, the added predictive value of imaging tools needs to be carefully evaluated in future research, taking into account the additional healthcare costs involved.

REFERENCES

1. Walsh PC: Anatomic radical retropubic prostatectomy. In Campbell's Urology, 7th ed., edited by Walsh PS, Retik AB, Vaughan ED Jr., Wein AJ, 3: 256588. Philadelphia: W. B. Saunders, 1998.

2. Walsh PC, Lepor H, Eggleston JC: Radical prostatectomy with preservation of sexual function: anatomical and pathological considerations. Prostate 4: 473–485, 1983

3. Rabbani F, Stapleton AMF, Kattan MW et al: Factors predicting recovery of erections after radical prostatectomy. J Urol 164: 1929–1934, 2000

4. Patel VR, Schatloff O, Chauhan S, et al: The role of the prostatic vasculature as a landmark for nerve sparing during robotassisted radical prostatectomy. Eur Urol 61: 571–576, 2012

5. Schatloff O, Chauhan S, Sivaraman A, et al: Anatomic grading of nerve sparing during robotassisted radical prostatectomy. Eur Urol 61: 796–802, 2012

6. Moskovic DJ, Alphs H, Nelson CJ, et al: Subjective characterization of nerve sparing predicts recovery of erectile function after radical

prostatectomy: defining the utility of a nerve sparing grading system. J Sex Med 8: 255–260, 2011

7. Briganti A, Gallina A, Suardi N, et al: Predicting erectile function recovery after bilateral nerve sparing radical prostatectomy: a proposal of a novel preoperative risk stratification. J Sex Med 7: 2521–2531, 2010

8. Levinson AW, Pavlovich CP, Ward NT, et al: Association of surgeon subjective characterization of nerve sparing quality with potency following laparoscopic radical prostatectomy. J Urol 179: 1510–1514, 2008

9. Schatloff O, Chauhan S, Kameh D, et al. Cavernosal nerve preservation during robot-assisted radical prostatectomy is a graded rather than an all-or-none phenomenon: objective demonstration by assessment of residual nerve tissue on surgical specimens. Urology 79: 596–600, 2012

10. Roumiguié M, Beauval JB, Filleron T, et al : External validation of the Briganti nomogram to estimate the probability of specimenconfined disease in patients with high risk prostate cancer. BJU Int 114: E113–E119, 2014

11. Partin AW, Kattan MW, Subong EN, et al: Combination of prostatespecific antigen, clinical stage, and Gleason score to predict pathological stage of localized prostate cancer. A multi institutional update. JAMA 277: 1445–1451, 1997

12. Kattan MW, Stapleton AM, Wheeler TM, et al: Evaluation of a nomogram used to predict the pathologic stage of clinically localized prostate carcinoma. Cancer 79: 528–537, 1997

13. Briganti A, Larcher A, Abdollah F, et al: Updated nomogram predicting lymph node invasion in patients with prostate cancer undergoing extended pelvic lymph node dissection: the essential importance of percentage of positive cores. Eur Urol 61: 480–487, 2012

14. Magi-Galluzzi C, Evans AJ, Delahunt B, Epstein JI, Griffiths DF, van der KwastTH, Montironi R, Wheeler TM, Srigley JR, Egevad LL, Humphrey PA; ISUP Prostate Cancer Group. International Society of Urological Pathology (ISUP) Consensus Conference on Handling and Staging of Radical Prostatectomy Specimens. Working group 3: extraprostatic extension, lymphovascular invasion and locally advanced disease. Mod Pathol 24: 26-38, 2011

15. Calle ML, Urrea V, Boulesteix AL, et al: AUCRF: A New Strategy for Genomic Profiling with Random Forest. Human Heredity 72: 121–132, 2011

16. Breiman L: Random forests. Mach Learn 45 :5–32, 2001

17. Ishwaran H, Kogalur UB, Gorodeski EZ, et al: High dimensional variable selection for survival data. J Am Stat Assoc 105: 205–217, 2010

18. Coste J, Pouchot J: A grey zone for quantitative diagnostic and screening tests. Int J Epidemiol 32: 304–313, 2003

19. Ploussard G, Agamy MA, Alenda O, et al: Impact of positive surgical margins on prostatespecific antigen failure after radical prostatectomy in adjuvant treatmentnaïve patients. BJU Int 107: 1748–1754, 2011

20. Godoy G, Tareen BU, Lepor H: Site of positive surgical margins influences biochemical recurrence after radical prostatectomy. BJU Int 104: 1610–1614, 2009

21. Maubon T, Branger N, Bastide C, et al: Impact of the extent of extraprostatic extension defined by Epstein's method in patients with negative surgical margins and negative lymph node invasion. Prostate Cancer Prostatic Dis 19: 317-21, 2016

22. Wheeler TM, Dillioglugil O, Kattan MW, et al: Clinical and pathological significance of the level and extent of capsular invasion in clinical stage T12 prostate cancer. Hum Pathol 29: 856–862, 1998

23. Kattan, MW, Eastham, JA, Stapleton AM, et al: A preoperative nomogram for disease recurrence following radical prostatectomy for prostate cancer. J Natl Cancer Inst 90: 766–771, 1998

24. Kattan MW, Zelefsky MJ, Kupelian PA, et al: Pretreatment nomogram for predicting the outcome of threedimensional conformal radiotherapy in prostate cancer. J Clin Oncol 18: 3352–3359, 2000

25. Ohori M, Kattan MW, Koh H, et al: Predicting the presence and side of extracapsular extension: a nomogram for staging prostate cancer. J Urol 171: 1844–1849, 2004

26. Steuber T, Graefen M, Haese A, et al: Validation of a nomogram for prediction of side specific extracapsular extension at radical prostatectomy. J Urol 175: 939–944, 2006

27. de Rooij M, Hamoen EH, Witjes JA, et al: Accuracy of Magnetic Resonance Imaging for Local Staging of Prostate Cancer: A Diagnostic Meta-analysis. Eur Urol 70: 233-45, 2016

28. Wang L, Hricak H, Kattan MW, Chen HN, Scardino PT, Kuroiwa K. Prediction of organ-confined prostate cancer: incremental value of MR imaging and MR spectroscopic imaging to staging nomograms. Radiology 238: 597-603, 2006

29. Gupta RT, Faridi KF, Singh AA, Passoni NM, Garcia-Reyes K, Madden JF, Polascik TJ. Comparing 3-T multiparametric MRI and the Partin tables

to predict organ-confined prostate cancer after radical prostatectomy. Urol Oncol 32: 1292-1299, 2014

30. Feng TS, Sharif-Afshar AR, Wu J, Li Q, Luthringer D, Saouaf R, Kim HL. Multiparametric MRI Improves Accuracy of Clinical Nomograms for Predicting Extracapsular Extension of Prostate Cancer. Urology 86: 332-337, 2015

31. Cerantola Y, Valerio M, Kawkabani Marchini A, et al: Can 3T multiparametric magnetic resonance imaging accurately detect prostate cancer extracapsular extension? Can Urol Assoc J 7: E699–E703, 2013

32. Xylinas E, Yates DR, Renard-Penna R, et al. Role of pelvic phased array magnetic resonance imaging in staging of prostate cancer specifically in patients diagnosed with clinically locally advanced tumours by digital rectal examination. World J Urol 31: 881–886, 2013

33. Rosenkrantz AB, Chandarana H, Gilet A, et al. Prostate cancer: utility of diffusion-weighted imaging as a marker of sidespecific risk of extracapsular extension. J Magn Reson Imaging 2013; 38: 312–319.

34. Kim CK, Park SY, Park JJ, et al. Diffusion-weighted MRI as a predictor of extracapsular extension in prostate cancer. AJR Am J Roentgenol 202: W270–W276, 2014

35. Woo S, Cho JY, Kim SY, et al. Extracapsular extension in prostate cancer: added value of diffusion-weighted MRI in patients with equivocal findings on T2-weighted imaging. AJR Am J Roentgenol 204: W16875, 2015

Table 1. Clinico-pathological characteristics of the 6,360 patients considered in the study

No of patients, n (%)	6360
Age (yrs)	62.0 (56.0 - 67.0)
BMI (kg/m2)	27.8 (25.4 - 30.5)
Race	
Caucasian	5717 (89.9)
Black	489 (7.7)
Other	154 (2.4)
PSA total (ng/mL)	5.0 (4.0 - 7.0)
PSA total (ng/mL)	
<10	5601 (88.1)
10-20	625 (9.8)
>20	128 (2)
PSA density (ng/mL/cc)	0.10 (0.07 - 0.15)
Prostate volume (cc)	15.0 (5.0 - 20.0)
Clinical stage (digital rectal examination), n (%)	
T1	4949 (77.9)
T2a	969 (15.3)
T2b	249 (3.9)
T2c	134 (2.1)
T3-T4	52 (0.8)
Biopsy Gleason sum, n (%)	
5 or less	6 (0.1)
6	3022 (47.6)
7	2588 (40.7)
8	485 (7.6)
9-10	253 (4)
Biopsy cores, n (%)	
6	701 (11)
7-11	369 (5.8)
12	4812 (75.7)
13-17	283 (4.4)
>17	195 (3.1)
Pathological stage, n (%)	
pT2a	560 (8.8)
pT2b	32 (0.5)
pT2c	3965 (62.3)
pT3a	1365 (21.5)
pT3b	438 (6.9)
Positive surgical margin (%)	917 (14.4)

Table 2. Multivariable logistic models to predict extracapsular extension on each side of the prostate gland; odds ratios (ORs) with confidence intervals (95% CI) and P-value of the likelihood-ratio test

	ECE		ECE > 1mm		ECE > 2mm		ECE > 3mm		ECE > 4mm	
	OR (95% CI)	P	OR (95% CI)	P	OR (95% CI)	P	OR (95% CI)	P	OR (95% CI)	P
Age	1.04 (1.03 - 1.05)	<0.001	1.06 (1.04 - 1.07)	<0.001	1.04 (1.02 - 1.06)	<0.001	1.04 (1.02 - 1.07)	0.001	1.05 (1.02 - 1.08)	<0.001
Log10(Total PSA)	4.31 (3.34 - 5.58)	<0.001	6.16 (4.31 - 8.79)	<0.001	8.64 (5.55 - 13.46)	<0.001	8.70 (5.01 - 15.12)	<0.001	7.59 (4.00 - 14.41)	<0.001
Clinical stage		<0.001		<0.001		<0.001		0.001		<0.001
T2a	1.41 (1.20 - 1.66)		1.84 (1.46 - 2.32)		2.11 (1.54 - 2.88)		1.75 (1.15 - 2.68)		2.42 (1.45 - 4.03)	
T2b	2.01 (1.54 - 2.61)		1.81 (1.26 - 2.59)		2.52 (1.63 - 3.91)		2.38 (1.37 - 4.16)		3.22 (1.67 - 6.19)	
T2c	1.24 (0.85 - 1.81)		1.71 (1.05 - 2.79)		2.27 (1.25 - 4.11)		2.53 (1.25 - 5.13)		4.05 (1.87 - 8.8)	
T3 - T4	1.68 (0.95 - 2.95)		2.64 (1.38 - 5.04)		4.59 (2.27 - 9.29)		4.07 (1.74 - 9.5)		4.34 (1.59 - 11.8)	
Rate of positive cores	3.48 (2.57 - 4.72)	<0.001	1.67 (1.05 - 2.65)	0.029						
Rate of cores with Gleason > 6	3.04 (2.60 - 3.54)	<0.001	2.92 (2.29 - 3.72)	<0.001	2.68 (1.92 - 3.73)	<0.001	3.23 (2.06 - 5.06)	<0.001	3.70 (2.12 - 6.49)	<0.001
Rate of cores with more than 60% of tumor	2.86 (2.06 - 3.97)	<0.001	2.15 (1.35 - 3.45)	0.001						

	ECE		ECE > 1mm		ECE > 2mm		ECE > 3mm		ECE > 4mm	
	OR (95% CI)	P	OR (95% CI)	P	OR (95% CI)	P	OR (95% CI)	P	OR (95% CI)	P
positive										
Mean rate of tumor positive	3.68 (1.89 - 7.18)	<0.001	6.55 (2.67 - 16.09)	<0.001	19.74 (11.05 - 35.27)	<0.001	21.69 (10.51 - 44.74)	<0.001	16.30 (6.86 - 38.72)	<0.001

[ECE, extracapsular extension; Pct., = percent]
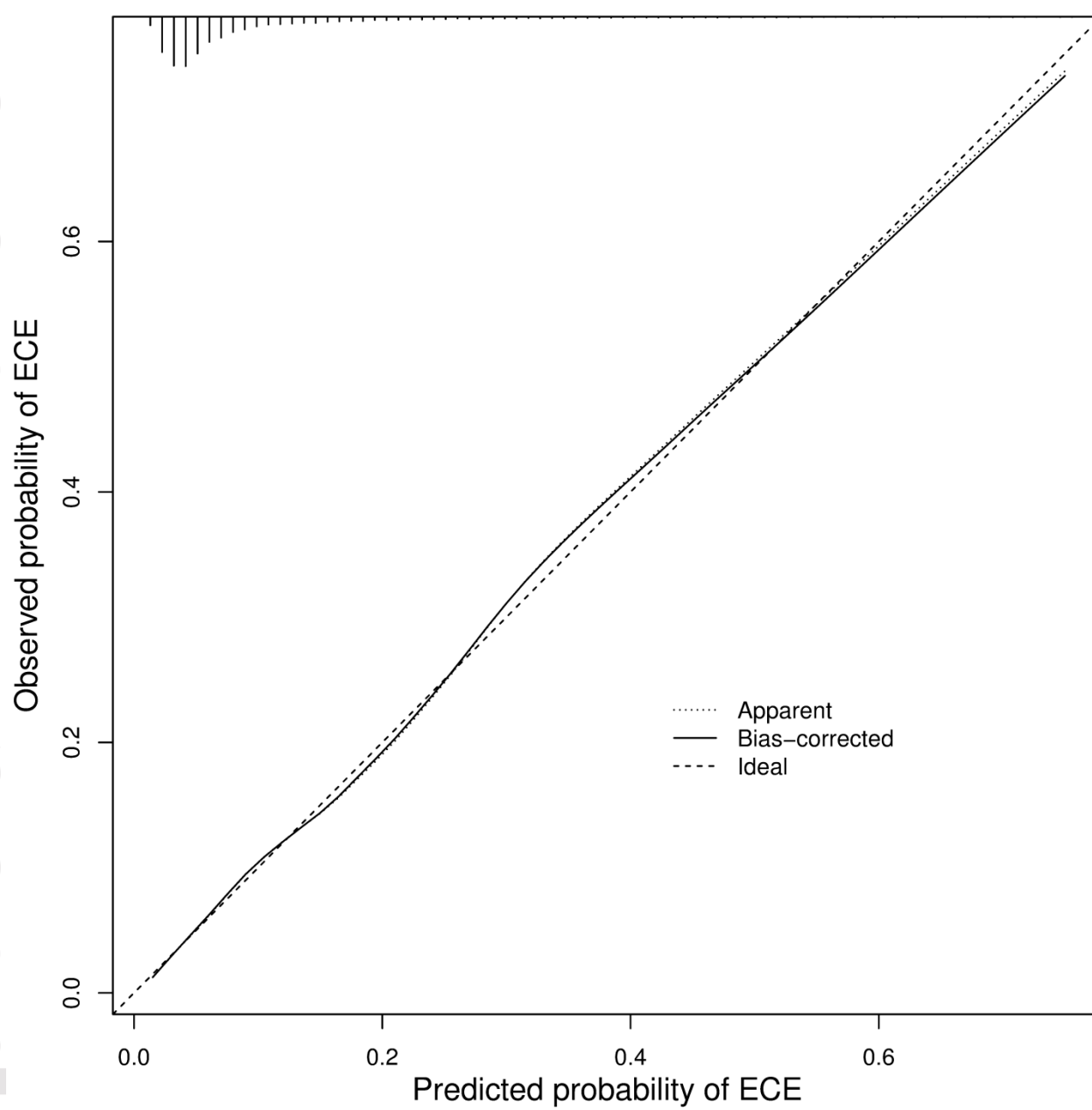
Figure 1.
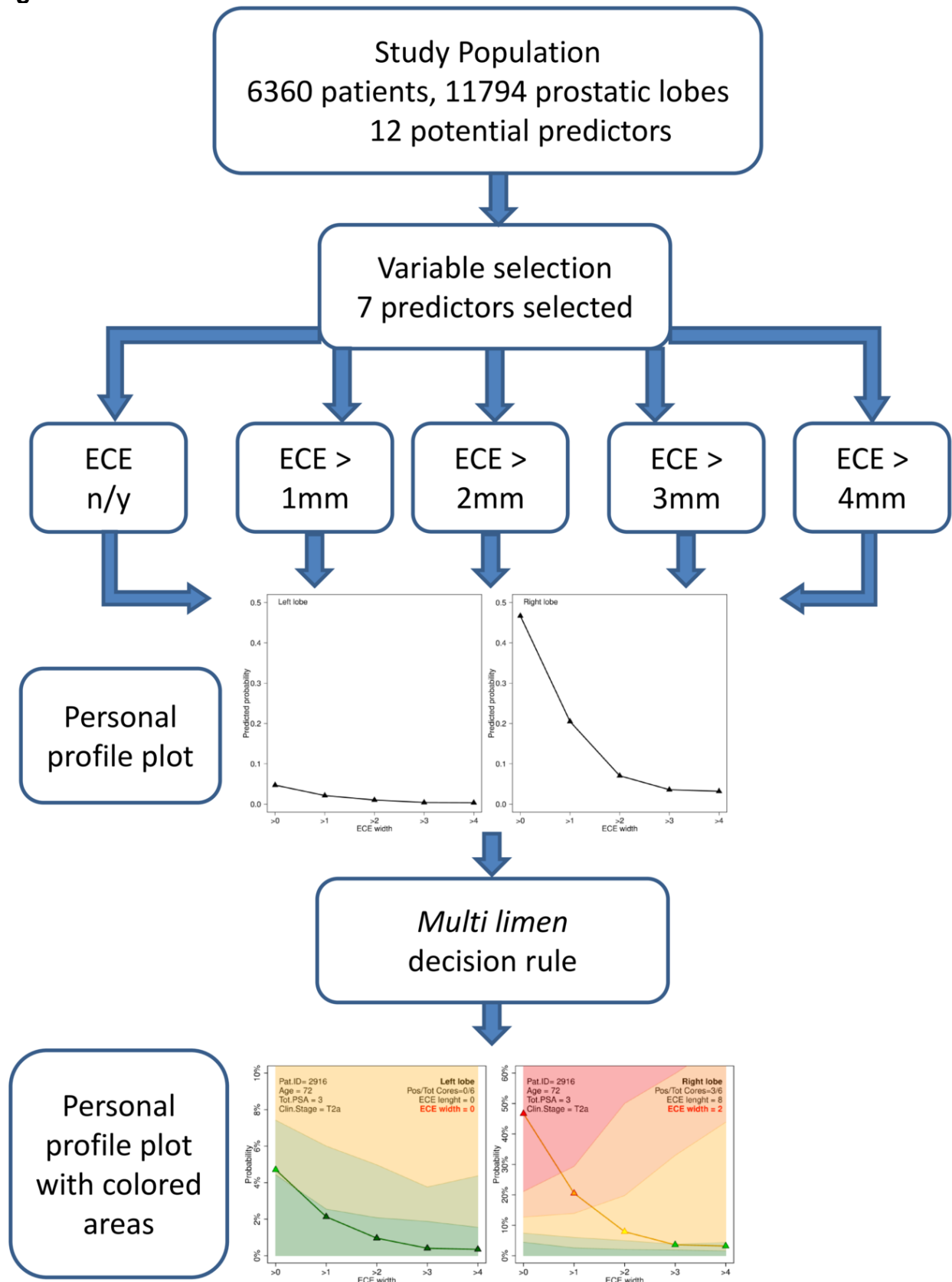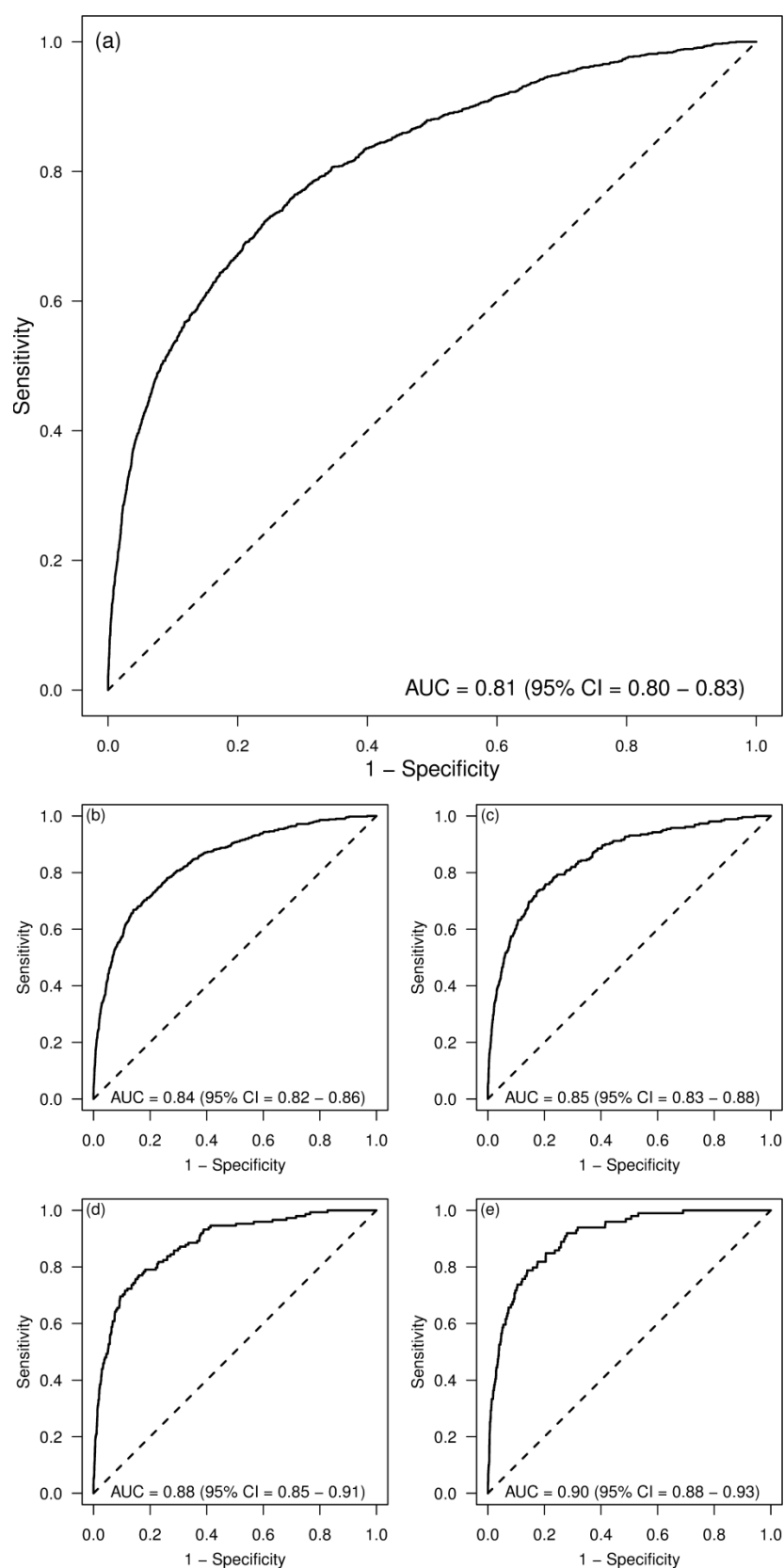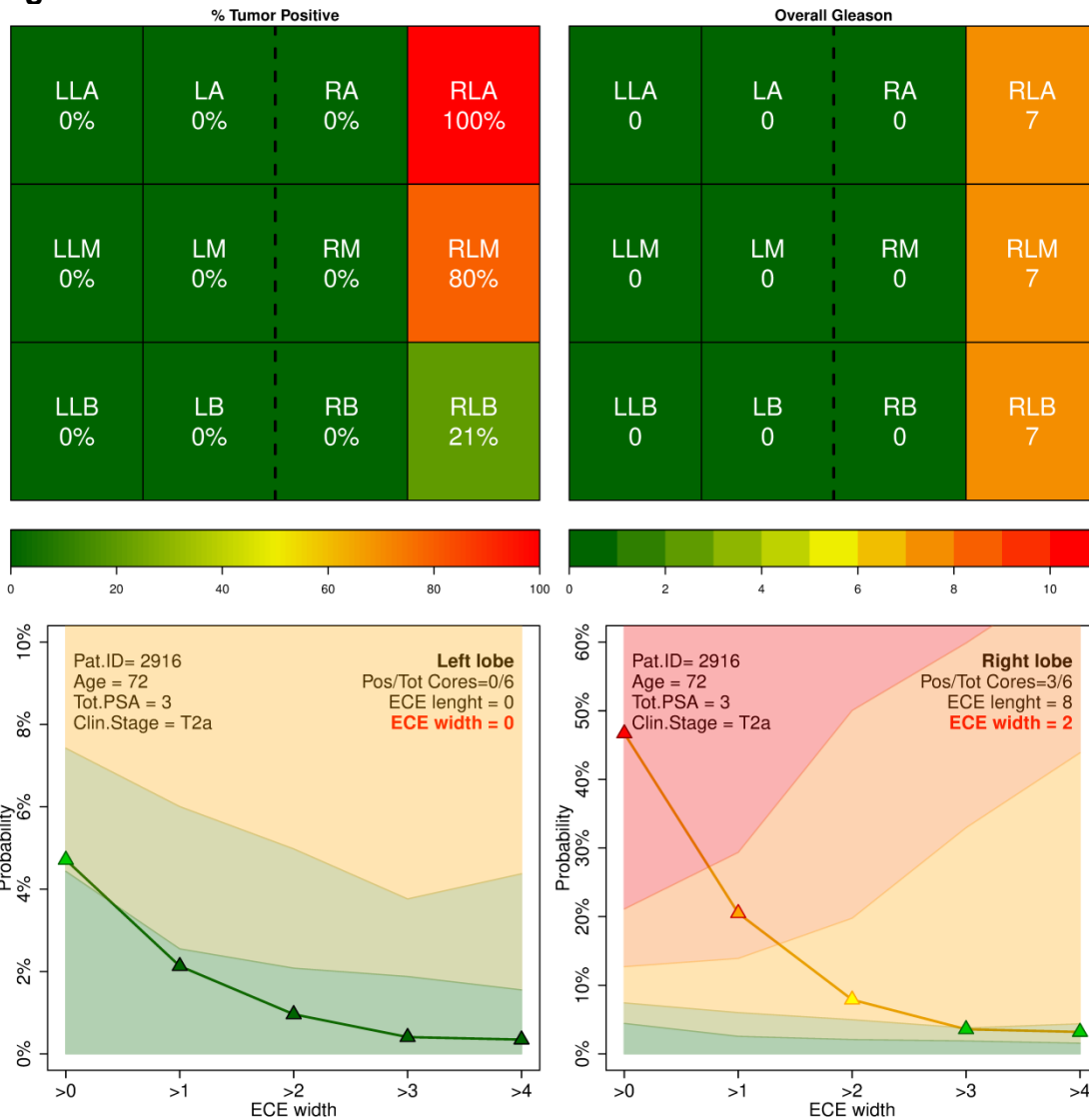
Figure 2.

Figure 3.

Figure 4

Pat.ID, patient identifier; Tot.PSA, total PSA (ng/mL); Clin.Stage, clinical stage; Pos/Tot Cores, rate between positive and total biopsy cores; LLA= left lateral apex; LA= left apex; RA= right apex; RLA= right lateral apex; LLM= left lateral median; LM= left median; RM= right median; RLM= right lateral median; LLB= left lateral base; LB= left base; RB= right base; RLB= right lateral base.